Available online at www.sciencedirect.com

ScienceDirect

Materials Today: Proceedings 5 (2018) 21574–21583

materialstoday: PROCEEDINGS

www.materialstoday.com/proceedings

The 3rd International Conference on Green Chemical Engineering Technology (3rd GCET_2017): Materials Science

Adsorption of Pb(II) onto KCC-1 from aqueous solution: Isotherm and kinetic study

R. Hasan[a], S.N. Bukhari[a], R. Jusoh[a], N.S.A. Mutamin[a], H.D. Setiabudi[a,b,*]

[a] *Faculty of Chemical and Natural Resources Engineering, Universiti Malaysia Pahang, 26300 Gambang, Kuantan, Pahang, Malaysia.*
[b] *Centre of Excellence for Advanced Research in Fluid Flow, Universiti Malaysia Pahang, 26300 Gambang, Kuantan, Pahang, Malaysia.*

Abstract

In this study, the removal of Pb(II) from aqueous solution using KCC-1 was investigated. BET and TEM revealed the favourable structure of KCC-1 which consists of fibrous morphology and high surface area (298.87 m^2/g). Batch adsorption experiment were performed to study the effects of contact time (40 – 160 min), adsorbent dosage (0.5 – 5g/L), initial concentration (50 – 400 mg/L) and pH (2 – 8) on the removal of Pb(II). The optimum condition was achieved at contact time of 80 min, adsorbent dosage of 4 g/L, initial concentration of 200 mg/L and pH of 6, with maximum removal of Pb(II) was 80.5%. The experimental data were analysed using Langmuir (Type 1, Type 2, Type 3 and Type 4), Freundlich, Temkin, and Dubinin-Redushkevich isotherm models, and were found to follow Langmuir isotherm model with maximum adsorption capacity of 38.76 mg/g and high correlation coefficient (R^2 = 0.99), implying that the ongoing process is homogeneous in nature. Pseudo-first-order, Pseudo-second-order, Intra-particle diffusion and Elovich kinetic models were tested with the experimental data, and Pseudo-second order kinetic model was the best for the adsorption of Pb(II) onto KCC-1, indicating that the adsorption process most likely be controlled by the chemisorption process and the rate of reaction is directly proportional to the number of active sites on the surface of adsorbent. The results obtained from this study revealed that KCC-1 has high potential for the adsorption adsorption of Pb(II) from aqueous solution.

Selection and/or Peer-review under responsibility of The 3rd International Conference on Green Chemical Engineering and Technology (3rd GCET): Materials Science, 07-08 November 2017.

Keywords: Adsorption; KCC-1; Pb(II); Kinetics; Isotherm

* Corresponding author. Tel.: +6-09-549-2836; fax: +6-09-549-2889.
E-mail address: herma@ump.edu.my

Selection and/or Peer-review under responsibility of The 3rd International Conference on Green Chemical Engineering and Technology (3rd GCET): Materials Science, 07-08 November 2017.

1. Introduction

Nowadays, water pollution associated with the heavy metals has become one of the most concerns especially in industrial country as the result of industrialization and technology development [1–3]. Industry activities including mining, agriculture and manufacturing usually release heavy metals that cannot be decomposed easily, and thus can cause adverse human and ecological health impacts. Lead (Pb(II)) is widely used in the manufacturing activities of alloys, pigments, cables, plastics, paints, fertilizer and batteries [1–3] have been ranked as second in the list of prioritised hazardous substances. Pb(II) has been recognised as a highly toxic heavy metal due to its tendency to accumulate in tissues of living organisms even in low concentration [1–3]. The exposure of high Pb(II) content to human is capable to cause severe damage to the brain, liver, kidney, reproductive system and nervous system [4,5]. Therefore, it is essential to reduce Pb(II) concentrations to permission standard before discharging them into the environment. Several organisations have set the maximum acceptable limit of Pb(II) in wastewater and the maximum permissible level of Pb(II) allowed by World Health Organization (1984) in drinking water is 0.05mg/L [6].

Various processes such as chemical precipitation [7], adsorption [3,5,8–10], coagulation [11], membrane [12], solvent extraction [13] and ion exchange [14] have been studied in removal process of Pb(II). Among others, adsorption is considered as an attractive method because of its high efficiency for the removal of Pb(II) from dilute solutions, inexpensive and simplicity in design [15–17]. Various adsorbents have been investigated for adsorption of Pb(II) including agriculture waste [18–21], activated carbon [3,4,15,20] and nanomaterial [17, 22–24].

During the past few years, a considerable amount of research have been devoted to the removal of Pb(II) using mesoporous silica materials due to their high potential towards the adsorption of organic and inorganic compounds [24–28]. Mesoporous silica such as MCM-48, MCM-41, HMS and SBA-15 have been used as an adsorbent because of their large surface area, narrow pore size distributions and controlled pore sizes. In brief, large surface area increased the accessible adsorption sites for high adsorption capacities, while, the narrow pore size distributions and controlled pore sizes allow this material controlled the accessibility for large molecules and improved access of target molecules [29]. This verified that superior structural properties of mesoporous silica might trigger the stronger effect of adsorption, indicating a weaker diffusion resistance to adsorbent molecule due to the formation of higher surface area, meanwhile larger pore size of adsorbent might increase the diffusion of target molecule to the internal pore structure of the catalyst. It was in agreement with Karim et al. [23] who had investigated the influence of high surface area with enormous pores of mesoporous silica nanoparticles over amino modified mesostructured silica nanoparticles (MSN_{AP}) on the methylene blue (MB) removal. They reported that the superior structure of MSN_{AP} was probably due to higher number of active sites provided on the MSN_{AP} surface, and thus triggered towards fast adsorption capacity. Besides, it is also noteworthy that the presence of Si-O and Si-OH groups on the mesoporous silica surface significantly triggered the formation of negatively charge density [22], indicating the creation of more sites for the adsorption of molecular ions.

Recently fibrous silica nanosphere (KCC-1) attracted considerable attention for various type of applications such as CO_2 capture-conversation [30], sensing [31], and extraction of ions [32] due to high surface areas, fibrous surface morphology with the dendrimeric silica fibers, wide pore diameter, high mechanical and thermal stability [24]. Fihri et al. [33] reported that high surface area of KCC-1 with dendrimeric morphology had triggered towards better Ru particles dispersion and led towards superior hydrogenolysis process with no deactivation up to eight days of the reaction. Besides, Huang et al. [34] mentioned that a higher adsorption capacity of salmon DNA over KCC-1 based nanomaterials as compared to MCM-41 based nanomaterials with functionalized of different organoamine groups on different part of their surface due to the large pores, wide pore mouths, fibrous pore network and high accessibility with an amenable structure of the catalyst. An excellent catalytic performance was also possessed by KCC-1 towards CO_2 methanation whereby it produced 38.9% of CH_4 which was five-fold higher than MCM-41 due to spherical morphology with larger particle size of dendritic fiber (200-400 nm) and higher surface area (773 m^2/g) [35]. Apart from that, KCC-1 is expected to perform very well especially in wastewater treatment owing to its favourable properties. Here, we further study the potential of KCC-1 as an alternative adsorbent for the removal of Pb(II), owing to its excellent structural properties. It is expected that a higher removal rate of heavy metal ion adsorption can be achieved using KCC-1 as an adsorbent.

2. Materials and Methods

2.1. Preparation of KCC-1

KCC-1 was prepared according to the method reported by Polshettiwar et al. [36]. In brief, 2.6 g of tetraethyl orthosilicate (TEOS, Merck) was dissolved in solution containing 30 mL of toluene (Merck), 1.5 mL of butanol (Merck), 1 g of cetyltriammonium bromide (CTAB, Aldrich), 0.6 g of urea (Merck) and 30 mL of water. The mixture was stirred for 45 min at room temperature followed by heating at 120ºC for 5 h in a teflon-sealed hydrothermal reactor. Then, the solution was centrifuged, washed with distilled water, and followed by oven-dried at 100^{o}C for 12 h. The dried sample was calcined at 550ºC for 5 h in air to obtain KCC-1.

2.2. Characterization of KCC-1

The morphology of KCC-1 was characterized using transmission electron microscopy (TEM, Philips CM12). The sample was dispersed in acetone by sonication, and deposited on an amorphous, porous carbon grid. The Bruneuer-Emmett-Teller (BET) analysis was carried out using Micromeritics® at 77 K in order to identify the textural properties of KCC-1. The infrared spectra of KCC-1 before and after adsorption were obtained using Fourier-transform infrared (FTIR Spectrometer Nicolet iS5, Thermo Scientific). The samples were scanned over the range of 4000 – 500 cm^{-1} to identify the functional group of KCC-1 that might be involved in the adsorption process.

2.3. Adsorption experiments

A batch adsorption method was applied to carry out the adsorption process. Pb(II) stock solution with a concentration of 1000 mg/L was prepared by dissolving the accurate amount of Lead (II) nitrate ($Pb(NO_3)_2$, Sigma-Aldich) in deionized water, before being diluted to desired concentration (50-400 mg/L). The hydrochloric acid (HCl) or sodium hydroxide (NaOH) was used to adjust the pH (2-8) of the solution.

In brief, a specific amount of KCC-1 (0.5 – 5 g/L) was added in a 250 ml conical flask containing 200 ml of Pb(II) solution. The mixture was prepared under constant stirring at 200 rpm at room temperature (30ºC). The samples were withdrawn at appropriate time (0 – 140 min) and centrifuged at 3500 rpm for 2 minutes. The residuals of Pb(II) concentration were measured using UV-vis spectroscopy at 520 nm. Dithizone was used as reagent to give brick red color to the solution.

The amounts of Pb(II) adsorbed and Pb(II) removal percentage were calculated using following equation:

$$q_t = \left(\frac{C_o - C_t}{m}\right) \times V \tag{1}$$

$$\text{Removal}\,(\%) = \left(\frac{C_o - C_t}{C_o}\right) \times 100 \tag{2}$$

where q_t is the amount of Pb(II) adsorbed at any time (mg/g), V is the volume of the Pb(II) solution, m is the mass of KCC-1 used (g), C_o is the initial concentration (mg/L) and C_t is the liquid-phase concentration of Pb(II) solution at any time (mg/L).

2.4. Adsorption Kinetics

In this study, pseudo-first order [37], pseudo-second order [38], intraparticle diffusion [39] and Elovich kinetic [40] were used as kinetic models to determine the mechanism of the adsorption process. The linearized forms of the models are expressed as follow:

Pseudo-first-order model:

$$\log(q_e - q_t) = \log q_e - \frac{k_1}{2.303} t \tag{3}$$

Pseudo-second-order model: $$\frac{t}{q_t} = \frac{1}{k_2 q_e^2} + \frac{1}{q_e} t \quad (4)$$

Intraparticle diffusion: $$q_t = K_{dif} t^{0.5} + C \quad (5)$$

Elovich kinetic: $$q_e = \left(\frac{1}{\beta}\right) \ln(\alpha\beta) + \left(\frac{1}{\beta}\right) \ln t \quad (6)$$

where q_e (mg/g) is the amount of Pb(II) adsorbed at equilibrium, q_t (mg/g) is the amount of Pb(II) adsorbed at time t, k_1 (L/min) is the rate constant of pseudo-second order adsorption, k_2 (g/mg.min) is the rate constant of pseudo-second order adsorption, K_{dif} (mg/g·min$^{0.5}$) is the intraparticle diffusion model parameter, C (mg/g) is a parameter related to the boundary layer thickness, α (mg/(g.min)) is the adsorption rate constant and β (g/mg) is desorption constant during the experiment.

2.5. Adsorption Isotherm

Adsorption isotherm is important design to describe adsorption system practically and also describe mechanism of solutes interact with adsorbents, and is critical in optimizing the use of adsorbents. Langmuir (Type 1, Type 2, Type 3 and Type 4) [41], Freundlich [42], Temkin [43] and Dubinin-Radushkevich [44] models were used for analysing the experimental data. The linearized forms of these isotherms are expressed as below:

Langmuir (Type 1): $$\frac{C_e}{q_e} = \frac{1}{q_m K_L} + \frac{C_e}{q_m} \quad (7)$$

Langmuir (Type 2): $$\left(\frac{1}{q_e}\right) = \left(\frac{1}{q_m K_L}\right)\left(\frac{1}{C_e}\right) + \left(\frac{1}{q_m}\right) \quad (8)$$

Langmuir (Type 3): $$q_e = q_m - \left(\frac{1}{K_L}\right)\left(\frac{q_e}{C_e}\right) \quad (9)$$

Langmuir (Type 4): $$\frac{q_e}{C_e} = K_L q_m - K_L q_e \quad (10)$$

Freundlich: $$\log q_e = \log K_F + \frac{1}{n} \log C_e \quad (11)$$

Temkin: $$q_e = B \ln A + B \ln C_e \quad (12)$$

Dubinin-Radushkevich: $$\ln q_e = \ln q_m - K_{DR} \varepsilon^2 \quad (13)$$

where C_e is the Pb(II) concentration at equilibrium (mg/L), q_e is the adsorption capacity at equilibrium (mg/g), q_m is the maximum adsorption capacity (mg/g), K_L is the Langmuir constant (L/mg), K_F is the Freundlich equilibrium constant ((mg/g)(L/mg)$^{1/n}$)), n is an empirical constant, B is the Temkin constant, A is the Temkin equilibrium binding constant (L/g), K_{DR} is Dubinin-Radushkevich constant (mol^2/kJ^2) and ε is the Polanyi potential (J/mol), in which can be calculated from $\varepsilon = RT \ln (1+1/C_e)$, where R is gas constant (8.314 J/mol·K) and T is absolute temperature (K). The essential characteristic of the Langmuir isotherm can be expressed in term of the dimensionless constant separation factor, R_L, which is given by $R_L = 1/(1+K_L C_o)$ [3]. The R_L parameter is considered a more reliable indicator of the adsorption, which indicates the shape of the isotherm to be either unfavourable ($R_L > 1$), linear ($R_L = 1$), favourable ($0 < R_L < 1$) or irreversible ($R_L = 0$) [3].

3. Results and Discussion

3.1. Characterization of KCC-1

The TEM image of KCC-1 shown in Figure 1 revealed that the synthesized KCC-1 consists of sphere with fibrous morphology. The fibrous structure of KCC-1 provides good possibility for Pb(II) to be trapped and adsorbed into the surface of KCC-1. The BET surface area and pore volume of KCC-1 was 298.87 m^2/g and 0.3569 m^3/g, respectively.

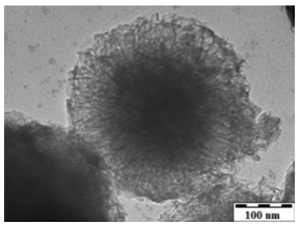

Fig. 1. TEM image of KCC-1.

The functional groups of KCC-1 before and after adsorption of Pb(II) were analysed using FTIR as shown in Figure 2. The FTIR spectrum of KCC-1 shows several absorbance bands approximately at 3399, 1062, 799 and 448 cm^{-1}. The band at 3399 cm^{-1} attributed to the O-H stretching vibration mode of Si-OH [45]. Meanwhile, the bands at 1062, 799 and 448 cm^{-1} assigned to the symmetrical stretching of Si-O, unsymmetrical stretching of Si-O and the bending of Si-O, respectively [45]. After the adsorption of Pb(II) onto KCC-1, the peaks at 3399, 1062, 799 and 448 cm^{-1} were slightly shifted to 3395, 1065, 800 and 450 cm^{-1}, respectively, indicating the interaction of Pb(II) with the functional groups of KCC-1. The shifted of peaks after the adsorption process was also reported by Beh et al. [9] for the removal of heavy metals from steel making waste water by using electric arc furnace slag. They reported that the shift of the peak could happen due to the complexation and coordination of functional group with metal ions.

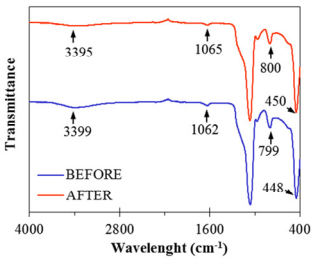

Fig. 2. FTIR before and after adsorption of Pb(II).

3.2. Batch Adsorption Study

3.2.1. Effect of Contact Time

The effect of contact time on the removal of Pb(II) onto KCC-1 is shown in Figure 2. The percentage removal of Pb(II) was increased with increasing of contact time until reached optimum condition at 80 min. Beyond 80 min, there was no increase in the Pb(II) removal and a steady-state approximation was assumed. The result shows that the Pb(II) removal was rapid in the first 80 min and constant until the end of the 140 min. The fast increasing at first of adsorption might be related to a high availability of active site on the surface of KCC-1, meanwhile the slower adsorption rate at the final stage might be due to the lowest active site on the surface of KCC-1[46]. This result was in agreement with the study reported by Moyo et al. [3] and Li et al. [27] for the adsorption of Pb(II) onto maize tassel based activated carbon and amino-functionalized fly-ash-based SBA-15, respectively. They claimed that the changes in the rate of Pb(II) removal with time was related to the availability of active sites on the surface of the adsorbent.

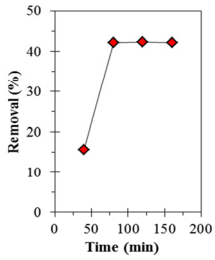

Fig. 3. Effect of contact time on Pb(II) adsorption onto KCC-1 (C_o = 50 mg/L, m_{KCC-1}= 0.5 g/L, pH = 6, T = 30ºC).

3.2.2. Effect of Adsorbent Dosage

Figure 3 shows the effect of KCC-1 dosage on Pb(II) removal. As shown in Figure 3, the percentage of removal increased significantly from 43.30% to 78.02%, with an increase in KCC-1 dosage from 0.1 g/L to 4 g/L and afterward remained unchanged with further increase in adsorbent dosage of KCC-1. This phenomenon can be due to an increase in availability of active site with an increase in adsorbent dosage and after the equilibrium is reached, the increasing of dosage will not much effect to the removal [47]. Similar trend reported by Guo et al. [28] for the adsorption of Pb(II) using chitosan-functionalized MCM-41-A. In their study, the adsorption of Pb(II) increase from 0.5 g/L to 2 g/L and afterwards remained unchanged with increasing of adsorbent dosage. They claimed that the changes in the adsorption process were related to the availability of active site on the surface of adsorbent due to the changes of adsorbent dosage.

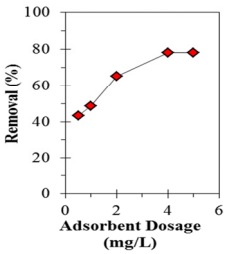

Fig. 4. Effect of adsorbent dosage of KCC-1 to the Pb(II) adsorption (C_o = 50 mg/L, pH = 6, T = 30ºC, t = 80 min).

3.2.3. Effect of Initial Concentration

The initial Pb(II) concentration was carried out in the concentration range of 50–400 mg/L (Figure 4). The percentage removal of Pb(II) increased markedly from 55.04% to 79.17% with an increase in Pb(II) concentration from 50–200 mg/L. However, further increase in Pb(II) concentration showed no significant changes in Pb(II) removal. The observed behaviour might be related to a decrease in the number of available active sites on the surface of KCC-1 with an increase in the amount of Pb(II) solution and thus, more Pb(II) will left in the solution [1]. Similar phenomenon reported by Javadian et al. [25] for nano HMS type mesoporous silica with N-(2-aminoethyl)-3-aminopropyl methyldimethoxysilane. They found that higher adsorption of Pb (II) was observed at low Pb(II) concentration, while further increasing in Pb(II) concentration slightly decreased the Pb(II) removal from 99.08% to 94.75%, due to a decreasing number of available active sites. Moreover, Guo et al. [28] also reported similar phenomenon for removal of Pb(II) over chitosan- functionalized functionalized MCM-41-A.

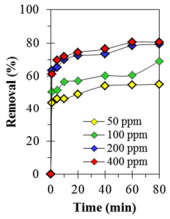

Fig. 5. Effect of concentration on Pb(II) onto KCC-1 (pH = 6, $m_{KCC\text{-}1}$= 4 g/L, T = 30 ºC, t = 80 min).

3.2.4. Effect of pH

Figure 5 indicates the effect of the pH on the removal of Pb(II) onto the KCC-1 with initial concentration of Pb(II) solution of 200 mg/L, adsorbent dosage of 4g/L with time of 80 min of adsorption process. The graph shows the removal of Pb(II) increased sharply at a lower pH until its maximum removal of Pb(II) was achieved at pH 6. However, the adsorption capacity of Pb(II) over KCC-1 was significantly decreased upon the increasing of pH value. Regarding to the previous study by Abbaszadeh et al. [4], increasing the pH might led to an excellent adsorption process due to the decreasing of competition between H^+ ions as the proton (acidic solution) and Pb(II) as cation. Meanwhile, a decrease in the adsorption process at pH 8 might be related to higher presence of excess H+ ions competing with the cations for the adsorption sites, and thus some precipitate of the solution might be formed at

pH above than 6 [48]. Zhou et al. [48] reported that the formation of precipitate in the aqueous solution was due to high concentration of hydroxyl group (−OH) that might be interacted with Pb(II) to form precipitate of $Pb(OH)_2$.

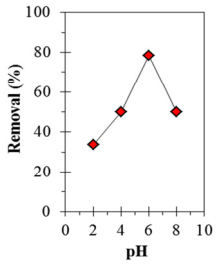

Fig. 6. Effect of pH on removal of Pb(II) onto KCC-1 (C_o = 200 mg/L, m_{KCC-1} = 4 g/L, T = 30 ºC, t = 80 min)`

3.3. Kinetic Study

Kinetic study explains the controlling mechanism of adsorption process to determine the equilibrium time and the mass transfer [46]. In treatment of aqueous effluent, the study of adsorption kinetic is important in order to provide the information on the adsorption process of Pb(II). The pseudo-first-order, pseudo-second-order, Intraparticle diffusion and Elovich kinetic model were used in this study to fit the experimental data. In detail, Pseudo-first order and pseudo second order explained the behaviour of adsorption which in physisorption or chemisorption, respectively, while, Elovich model will describe the kinetic of heterogeneous chemisorption and Intraparticle diffusion will explain the rate movement of metal ions from the Pb(II) solution to the surface of adsorbent [49,50].

The calculated data from each model was tabulated and summarized in Table 1. As observed from the data, the suitable model for this kinetic study of Pb(II) adsorption process over KCC-1 followed the order of Pseudo second order > intraparticle diffusion > pseudo-first-order > Elovich, indicating that pseudo-second-order described as the best fit with the experimental data whereby it exhibited the highest regression coefficient, R^2 ($\geq$ 0.9989) and close value of q_e than other models. Meanwhile, Elovich model represented as the weakest model for investigating the adsorption capacity of Pb(II) over KCC-1 due to the R^2 value $\leq$ 0.9. The highest value of R^2 and the close value of q_e towards pseudo-second-order indicated that the adsorption process most likely be controlled by the chemisorption process and the rate of reaction is directly proportional to the number of active sites on the surface of adsorbent. This result is in agreement with the changes in the FTIR bands after the adsorption process (Figure 2) which demonstrated the chemical interaction involved between Pb(II) and KCC-1 during the adsorption process. Comparable findings were also reported for the adsorption of Pb(II) onto novel Pb(II) ion-imprinted materials based on bis-pyrazolyl functionalized mesoporous silica [51], activated carbon adsorbent from locally available papaya peel biowaste [4], aqueous solution using nano-sized hydroxyapatite [46], and coal-based activated carbon [2]. They found that the experimental data followed the pseudo-second-order model indicating that the adsorption process controlled by a chemisorption process.

Table 1. Comparison of kinetic study.

Models	Parameter	50 ppm	100 ppm	200 ppm	300 ppm	400 ppm
Experimental	$q_{e,exp}$ (mg/g)	48.683	53.622	65.976	69.578	70.002
Pseudo-first-order	$q_{e,cal}$ (mg/g)	12.000	14.984	13.347	7.8656	12.283
	k_1 (min^{-1})	0.0486	0.0912	0.1004	0.0458	0.0529
	R^2	0.9179	0.8339	0.9587	0.9838	0.8368
Pseudo-second-order	$q_{e,cal}$ (mg/g)	48.781	52.083	66.225	69.444	70.423
	k_2 (g/mg·min)	0.0099	0.0088	0.0115	0.0148	0.0093
	R^2	0.9973	0.9913	0.9987	0.9989	0.9982
Intraparticle diffusion	K_{dif} ($mg/g.min^{0.5}$)	1.4344	1.4298	1.5568	0.8742	1.4527
	C (mg/g)	35.307	38.381	52.392	60.739	56.421
	R^2	0.9634	0.8832	0.9622	0.9312	0.9047
Elovich kinetic	α (mg/(g.min))	8E+05	2E+06	4E+07	1E+16	2E+09
	β (g/mg)	0.3605	0.3597	0.3199	0.6025	0.3651
	R^2	0.8617	0.7987	0.9273	0.8028	0.7693

3.4. Isotherm Study

Isotherm study was used to analyze the interaction between Pb(II) as adsorbate and KCC-1 as adsorbent. Four different types of isotherm model were used in this study; (1) Langmuir (Type 1, Type 2, Type 3 and Type 4), (2) Freundlich, (3) Temkin, and (4) Dubinin-Radushkevich isotherm. Langmuir isotherm is related with the relationship between the presence of active sites on the surface of adsorbent and the concentration of adsorbate in the solution at equilibrium. Once the adsorption of adsorbate onto the surface of adsorbent occurred, it might create a formation of monolayer on the homogenous surface of adsorbent which then affected towards no further adsorption [25]. Besides, Freundlich isotherm was commonly used for the multilayer adsorption over heterogeneous surface of adsorbent [52]. Meanwhile, Temkin isotherm was used to study the effect of adsorbate-adsorbent interactions in adsorption [25] and it was reported that these adsorbate-adsorbent interactions might produce a decreasing of heat adsorption of all molecules in the layer linearly due to coverage of adsorbent surfaces. Dubinin-Radushkevich isotherm was corresponded to an idea about the kind of adsorption depended on the activation energy such as the physisorption and chemisorption reaction involved between adsorbate and adsorbent [5].

The values of Langmuir (Type1, Type 2, Type 3 and Type 4), Freundlich, Temkin, and Dubinin-Radushkevich parameter were calculated using the formula and presented in Table 2. To quantitatively compare the accuracy of the models, the correlation coefficients (R^2) were also calculated and listed in Table 1. Analysis of the R^2 values suggests that Langmuir isotherm (Type 1) model better described the adsorption of Pb(II) onto KCC-1. This result indicates that the adsorption process might have taken place as monolayer adsorption on the homogenous surface of adsorbent in nature. According to Table 2, the Langmuir q_m value, K_L constant, R_L value was 38.760 mg/g, 0.0376 L/mg, and 0.2102, respectively. It confirmed that the prepared KCC-1 was significantly favourable for the Pb(II) adsorption under conditions used in this study. Langmuir isotherm was also reported as the best adsorption isotherm for the removal of Pb(II) onto Chitosan Beads [47], Maize Tassel Based Activated Carbon [3], and amino-functionalized fly-ash-based SBA-15 mesoporous molecular [27] with $R^2 \geq 0.9$, indicating the adsorption take place as monolayer on homogenous surface.

Table 2. Comparison of isotherm study.

Isotherm	Parameters	Value
Langmuir type 1	q_m (mg/g)	38.760
	K_L (L/mg)	0.0376
	R^2	0.9900
	R_L	0.2102
Langmuir type 2	q_m (mg/g)	40.161
	K_L (L/mg)	0.0403
	R^2	0.8441
	R_L	0.0473
Langmuir type 3	q_m (mg/g)	40.015
	K_L (L/mg)	0.0396
	R^2	0.9033
Langmuir type 4	q_m (mg/g)	37.711
	K_L (L/mg)	0.0360
	R^2	0.9033
Freundlich	n	2.1896
	K_f (mg/g)(L/mg)$^{1/n}$	444.43
	R^2	0.8768
Temkin	B (J/mol)	26.807
	A (L/g)	771.44
	R^2	0.8646
Dubinin-Radushkevich	q_m (mg/g)	47.224
	K_{ad} (10^{-4})	2
	R^2	0.7713

Table 3 shows the comparison of q_m value which was exhibited by KCC-1 in this study with other previous adsorbents. From the comparison, adsorption capacity of KCC-1 was higher than that of Thiophenecarbonyl Loaded

Silica Gel (TLSG), Activated Silica Gel (ASG), 2-Furoyl Loaded Silica Gel (FLSG) and L-Proline Loaded Silica Gel (PLSG) while lower than that of NH_2-MCM-41, Entrapped Silica Nanopowders, Chitosan-Functionalized MCM-41-A, and Fly Ash Based SBA-15. The higher adsorption capacity of KCC-1 as compared with some of the adsorbent listed in Table 3 might due to the fibrous morphology of the KCC-1. Even though the adsorption capacity of KCC-1 was lower than that of SBA-15 and MCM-1, KCC-1 still shows great potential to be used as alternative adsorbent for Pb(II) removal.

Table 3. Comparison of maximum adsorption capacity.

Adsorbent	Adsorption capacity (mg/g)	Ref
KCC-1	38.76	This study
Thiophenecarbonyl Loaded Silica Gel (TLSG)	17.85	[26]
Activated Silica Gel (ASG)	15.62	[26]
2-Furoyl Loaded Silica Gel (FLSG)	19.60	[26]
L-Proline Loaded Silica Gel (PLSG)	22.22	[26]
NH_2-MCM-41	57.74	[50]
Entrapped Silica Nanopowders	83.33	[8]
Chitosan-Functionalized MCM-41-A	90.91	[28]
Fly Ash Based SBA-15	121.0	[27]

4. Conclusion

In this piece of work, KCC-1 was prepared as adsorbent and used for removal of Pb(II). The optimum conditions were achieved at time of 80 min, adsorbent dosage of 4g/L, initial concentration of 200 mg/L, and initial pH of 6, with maximum removal of Pb(II) was 80.5%. The BET surface area and pore volume of KCC-1 was 298.87 m^2/g and 0.3569 m^3/g, respectively. TEM image of KCC-1 revealed the presence of fibrous morphology which provides good possibility for Pb(II) to be trapped and adsorbed into the surface of KCC-1. The equilibrium data for Pb(II) adsorption onto KCC-1 were modelled with the Pseudo-first-order, Pseudo-second-order, Intra-particle diffusion and Elovich kinetic models, and the data followed well the Pseudo-second-order kinetic model, which suggested that the adsorption process presumably controlled by chemisorption process and the reaction rate is directly proportional to the number of active sites on the surface of adsorbent. The result obtained in kinetic model in agreement with with the changes in the FTIR bands after the adsorption process (Figure 2) which demonstrated the chemical interaction involved between Pb(II) and KCC-1 during the adsorption process. The experimental data were also analysed using Langmuir (Type 1, Type 2, Type 3 and Type 4), Freundlich, Temkin, and Dubinin-Redushkevich isotherm models, and were found to follow Langmuir isotherm model with adsorption capacity 38.76 mg/g and correlation coefficient, R^2 of 0.99, indicating that KCC-1 surface is homogeneous in nature. The results obtained from this study revealed that KCC-1 has high potential for the adsorption of Pb(II) from aqueous solution.

Acknowledgement

The authors would like to express their deep gratitude to Universiti Malaysia Pahang (UMP) for providing the financial support through Research University Grant (RDU 170331).

References

[1] M.S. Rajput, A.K. Sharma, S. Sharma, S. Verma, Internaltional J. Appl. Res.1 (9) (2015) 411-413.
[2] Z. Yi, J. Yao, M. Zhu, H. Chen, F. Wang, X. Liu, Springerplus. 5 (1160) (2016) 1-12.
[3] M. Moyo, L. Chikazaza, B. C. Nyamunda, U. Guyo, J. Chem.. 2013 (2013) 1-8.
[4] S. Abbaszadeh, S.R. W. Alwi, C. Webb, N. Ghasemi, I. I. Muhamad, J. Clean. Prod.. 1 (2016) 15-45.
[5] A. Günay, E. Arslankaya, I. Tosun, J. Hazard. Mater. 146 (1-2) (2007) 362–371, 2007.
[6] World Health Organization, World Heal. Organ. Geneva, Switzerlandl. (1984) 1–2.
[7] A.M. Merganpour, G. Nekuonam, O.A. Tomaj, Y. Kor, H. Safari, Environ. Heal. Eng. Manag. J., 2 (1) (2015) 41-45.
[8] R.D.C. Soltani, G.S. Khorramabadi, A.R. Khataee, S. Jorfi, J. Taiwan Inst. Chem. Eng., 45 (3) (2014) 973–980.
[9] C.L. Beh, T.G. Chuah, M.N. Nourouzi, T. S. Y. Choong, J. Chem.. 9 (4) (2012) 2557-2564.
[10]S.A. Chaudhry, T.A. Khan, I. Ali, J. Mol. Liq. 236 (2017) 320-330.
[11]I.K. Shakir, B.I. Husein, Iraqi J. Chem. Pet. Eng. 10 (2009).
[12]H.A. Qdais, H. Moussa, Desalination. 164 (2) (2004) 105-110.

[13]D.B. Shah, A.V. Phadke, W.M. Kocher, J. Air Waste Manag. Assoc. 45 (3) (1995) 150-155.
[14]S. Rengaraj, K.-H. Yeon, S.-H. Moon, J. Hazard. Mater. 87 (1-3) (2001) 273-287.
[15]N. Chaouch, M. R. Ouahrani, S.E. Laouini, Orient. J. Chem. 30 (3) (2014) 1317-1322.
[16]N. Azouaou, M. Belmedani, H. Mokaddem, Z. Sadaoui, Chem. Eng. Trans. 32 (2013) 55-60.
[17]Y. Qi, M. Jiang, Y.-L. Cui, L. Zhao, X. Zhou, Nanoscale Res. Lett. 10 (1) (2015) 408.
[18]R.M. Novais, L.H. Buruberri, M.P. Seabra, J.A. Labrincha, J. Hazard. Mater. 318 (2016) 631-640.
[19]M.A.P. Cechinel, S.M.A.G. Ulson de Souza, A.A. Ulson de Souza, J. Clean. Prod. 65 (2014) 342-349.
[20]L. Largitte, J. Laminie, J. Environ. Chem. Eng. 3 (1) (2015) 474-481.
[21]N. Zhou, H. Chen, Q. Feng, D. Yao, H. Chen, H. Wang, Z. Zhou, H. Li, Y. Tian, X. Lu, J. Clean. Prod. 165 (2017) 221-230.
[22]M. Anbia, S. A. Hariri, Desalination. 261 (1-2) (2010) 61-66.
[23]A.H. Karim, A.A. Jalil, S. Triwahyono, S.M. Sidik, N.H.N. Kamarudin, R. Jusoh, N.W.C. Jusoh, H.H. Hameed, J. Colloid Interface Sci. 386 (1) (2012) 307-314.
[24]Z. Dong, X. Le, C. Dong, W. Zhang, X. Li, J. Ma, Appl. Catal. B Environ. 162 (2015) 371-380.
[25]H. Javadian, B.B. Koutenaei, E. Shekarian, F.Z. Sorkhrodi, R. Khatti, M. Toosi, J. Saudi Chem. Soc. 21 (2017) S219-S230.
[26]A.K. Kushwaha, N. Gupta, M.C. Chattopadhyaya, Arab. J. Chem. 10 (2017) S81-S89.
[27]G. Li, B. Wang, Q. Sun, W.Q. Xu, Y. Han, Microporous Mesoporous Mater. 252 (2017) 105-115.
[28]Y. Guo, D. Liu, Y. Zhao, B. Gong, Y. Guo, W. Huang, J. Taiwan Inst. Chem. Eng. 71 (2017) 537-545.
[29]T.Z. Ren, Z.Y. Yuan, B.L. Su, Colloids Surfaces A Physicochem. Eng. Asp. 300 (1-2 SPEC. ISS.) (2007) (79-87).
[30]B. Singh, V. Polshettiwar, J. Mater. Chem. A. 4 (18) (2016) 7071.
[31]M. Bouhrara, C. Ranga, A. Fihri, R.R. Shaikh, P. Sarawade, A.H. Emwas, M.N. Hedhili, ACS Sustain. Chem. Eng. 1 (9) (2013) 1192-1199.
[32]A. Aghakhani, E. Kazemi, M. Kazemzad, J. Nanoparticle Res. 17 (10) (2015) 1-13.
[33]A. Fihri, M. Bouhrara, U. Patil, D. Cha, Y. Saih, V. Polshettiwar, ACS Catal. 2 (7) (2012) 1425-1431.
[34]X. Huang, Z. Tao, J.C. Praskavich, A. Goswami, J.F. Al-Sharab, T. Minko, V. Polshettiwar, T.Asefa, Langmuir. 30 (36) (2014) 1088610898.
[35]M.Y.S. Hamid, M.I. Firmansyah, S. Triwahyoo, A.A. Jalil, R.R. Muktu, E. Febriyanti, V. Suendo, H. D. Setiabudi, M. Mohamed, Nabgan, Appl. Catal. A Gen. 532 (2017) 86-94.
[36]V. Polshettiwar, D. Cha, X. Zhang, J. M. Basset, Angew. Chemie - Int. Ed. 49 (50) (2010) 9652-9656.
[37]S. Lagergren, J. Chem. Eng., vol. 24, no. 1, pp. 1–39, 1898.
[38]Y.S. Ho, G. McKay, J. Process Biochem. 34 (5) (1999) 451-465.
[39]W.J. Weber, J.C. Morris, J. Sanit. Eng. Div. 89 (1963) 31-60.
[40]R.L. Tseng, F.C. Wu, R. S. Juang, Chem. Eng. J. 150 (2009) 366-373.
[41]I. Langmuir, J. Am. Chem. Soc. 40(9) (1918) 1361–1403.
[42]H. Freundlich, Adsorption in solution, J. Phys. Chem. 57 (1906) 47-385.
[43]M.M. Dubinin, Chem. Rev. 60 (1906) 235-266.
[44]M.I. Tempkin and V. Pyzhev, USSR. 12 (1940) 327-356.
[45]S. M. Sadeghzadeh, R. Zhiani, S. Emrani, RSC Adv. 7 (40) (2017) 24885-24894.
[46]S.T. Ramesh, N. Rameshbabu, R. Gandhimathi, M. Srikanth Kumar, P.V. Nidheesh, Appl. Water Sci. 3 (1) (2013) 105-113.
[47]G. Gyananath, D.K. Balhal, L. Sciences, Cellul. Chem. Technol. 46 (II) (2012) 121-124.
[48]T. Zhou, F. Xia, Y. Deng, Y. Zhao, J. Environ. Sci. 1 (II) (2017) 1-10.
[49]K. Riahi, S. Chaabane, B. Ben Thayer, J. Saudi Chem. Soc. 21 (2017) S143-S152.
[50]A. Heidari, H. Younesi, Z. Mehraban, Chem. Eng. J. 153 (1-3) (2009) 70-79.
[51]H. Z. Cui, Y.-L. Li, S. Liu, J.-F. Zhang, Q. Zhaou, R. Zhong, M.-L. Yang, X.-F. Hou, Microporous Mesoporous Mater. 241 (2017) 165-177.
[52]V. Srivastava, M. Shekhar, D. Gusain, F. Gode, Y.C. Sharma, Arab. J. Chem. 10 (2014) S3073-S3083.